Lifetimes and Oscillator Strength Trends For the 4s2nd2d Series of Ga I

Brage, Tomas; Fischer, C. F; Carlsson, J; Wahlström, Claes-Göran

Published in:
Physical Review A (Atomic, Molecular and Optical Physics)

DOI:
10.1103/PhysRevA.35.1113

1987

Lifetimes and oscillator strength trends for the $4s^2nd\ ^2D$ series of Ga I

T. Brage* and C. Froese Fischer†
Argonne National Laboratory, Argonne, Illinois 60441

J. Carlsson and C. -G. Wahlström
Department of Physics, Lund Institute of Technology, Lund, Sweden
(Received 2 July 1986)

Theoretical transition probabilities for kf-nd and mp-nd transitions in Ga I ($k=4$–6, $m=4$–7, and $n=4$–8) are reported together with lifetimes for the first five members of the $4s^2nd\ ^2D$ series. Mixing with $4s4p^2\ ^2D$ is found to be very important. The sensitivity of the $nd\ ^2D$ lifetimes to the position of this perturber is discussed, together with the oscillator strength trend for the transitions from the $nd\ ^2D$ series, $n=4$–11, to the ground state. The calculated lifetimes are in good agreement with recent laser experiments.

I. INTRODUCTION

Recent measurements of the lifetimes in Ga I of levels in the $4s^2nd\ ^2D$ series, using laser techniques,[1] show a strong divergence from the normal $(n^*)^3$ trend, where n^* is the effective principal quantum number.

Previous studies of the homologous Al I sequence[2] suggest that these irregularities are caused primarily by the interaction with the $4s4p^2\ ^2D$ configuration. Such sd-p^2 interactions are known to be strong from studies of other systems, e.g., Mg I–like ions.[3] We therefore expect that this configuration will have a large influence on the diffuse series, even though it has an energy about 5000 cm^{-1} above the ionization limit[4] (to be compared with a binding energy of about 13 000 cm^{-1} for the $4d$ electron in $4s^24d\ ^2D$). This implies that even though Ga I is essentially a one-electron system, with normal terms of the form $4s^2nl\ ^2L$, the "softness" of the $4s$ shell introduces correlation between the $4s$ and nl electrons.

Earlier calculations on the ^2D series either have treated only the lowest member[5,6] or have assumed a single-configuration approach.[7] For higher n values, semiempirical quantum-defect theory has been used to deduce the position of the perturber.[8]

From a theoretical point of view it can be argued that a perturber embedded in the continuum should give rise to a Beutler-Fano profile[9] in the transition probabilities, which can be extrapolated into the discrete Rydberg series. We also know from photoabsorption studies that the $msmp^2\ ^2D$ state, in group-III atoms, gives rise to a very broad resonance, and has been suggested to cause a minimum in transition probabilities around $n=9$ for Ga I and In I ($m=4$ and 5, respectively.)[10]

This minimum, which results from a cancellation effect (see below), causes the lifetimes of the ^2D states to be very sensitive to the contributions from transitions to the excited ^2P and ^2F states. Thus, to obtain reliable lifetimes of the higher ^2D states, a large number of states have to be included in the calculation.

In this paper we consider (a) lifetimes for $4s^2nd\ ^2D$, $n=4$–8, and (b) the oscillator-strength trend for the $4s^24p\ ^2P$–$4s^2nd\ ^2D$ transitions, $n=4$–11.

II. METHOD OF CALCULATION

Wave functions were obtained using the multiconfiguration Hartree-Fock (MCHF) package[11] in a frozen-core approximation, where the $1s$, $2s$, $2p$, $3s$, $3p$, and $3d$ orbitals were taken from a Hartree-Fock calculation of the ground state, $4s^24p\ ^2P$. The wave-function expansions for each state are summarized in Table I, where only orbitals with the same indices are orthogonal, and the orbitals without indices are orthogonal to all one-electron functions with the same orbital quantum number l. For example, $4p_1$ and $5p_1$ are orthogonal, and so are $3d$ and $4d_1$, but not $4d_1$ and $4d_2$. Test calculations have shown that the core polarization has only a limited effect on the transition probabilities and therefore is not included in the final calculations.

A. p states

To get convergence for the $np\ ^2P$ states, we had to change the expansion in going from the ground state to the excited states by including some lower-lying configuration states of the same symmetry. In the calculations for the $5p$ state we included $4s_1^24p_1$, as obtained from a Hartree-Fock calculation of the ground state, without optimizing the corresponding $4p_1$ orbital during the MCHF procedure. In the calculations for $6p$, $4p_2^2(^1S)5p_2$ was included, together with the lower $4s_1^24p_2$ and $4s_1^25p_2$ configuration states. In the optimization of this state the $4p_2$ and $5p_2$ orbitals were kept fixed. Since test calculations showed that the np orbitals were very similar in $4s^2np$ and $4p^2(^1S)np$, the same orbital, labeled np_2, was used in both cases for the higher states ($n=6$ and 7). Calculations for the $7p$ state were performed in a similar manner as for the $6p$ state (see Table I). Instead of calculating the $8p$ state, an extrapolation of the probabilities for np-nd transitions was used to obtain a value for the $4s^28p\ ^2P$–$4s^28d\ ^2D$ transition probability.

B. d states

Since the ^2D states were much more stable than the ^2P states, no lower members of the Rydberg series had to be

TABLE I. Wave-function expansions.

A. $4s^2np\ ^2P$

Part 1. n-dependent basis set

(i) $(4s_1^2+4d_1^2+4f_1^2)(^1S)np_1\ ^2P$

(ii) $4p_2^2(^3P,^1D,^1S)np_2\ ^2P$

$n=4$: (ii) is replaced by $4p_2^3\ ^2P+4p_2^2(^1S)5p_2\ ^2P$ and $4d_1^2(^3P,^1D)4p_1\ ^2P$ is added.

$n=6,7$: np_1 is replaced by np_2.

Part 2. Common to all

(iii) $4s_15s_1(^3S,^1S)4p_3\ ^2P+4p_2^2(^1D)4f_2\ ^2P+4s_14p_3(^3P,^1P)4d_2\ ^2P$ $+4s_14d_3(^3D,^1D)4f_2\ ^2P$

Part 3. Lower state of same symmetry

$n=5$: $4s_1^24p_1\ ^2P$

$n=6$: $4s_1^2np_2\ ^2P$ for $n=4,5$; $4p_2^25p_2\ ^2P$

$n=7$: $4s_1^2np_2\ ^2P$ for $n=4$–6; $4p_2^2np_2\ ^2P$ for $n=5,6$

B. $4s^2nd\ ^2D$

$(4s_1^2+4p_1^2+4d_1^{2*}+4f_1^2)(^1S)nd_1\ ^2D+4s_15s_1(^3S,^1S)nd_2\ ^2D$ $+4s_2(4p_2^2+4d_2^2+4f_3^2)(^1D)^2D+4p_25p_2(^3D)4s_2\ ^2D$ $+4p_34f_2(^3D,^1D)4s_2\ ^2D+4p_44d_4(^3F,^3D,^3P,^1F,^1D,^1P)4f_4\ ^2D$ $+4p_2^2(^3P,^1D)4d_5\ ^2D$

*In $4s^24d\ ^2D$ we have used $4d_6^3\ ^2D+4d_6^25d_6\ ^2D$

C. $4s^2nf\ ^2F$

$(4s_1^2+4p_1^2+4d_1^2+4f_1^{2*})(^1S)nf_1\ ^2F+4s_24p_2(^3P,^1P)4d_2\ ^2F$ $+4s_24d_3(^3D,^1D)4f_2\ ^2F$

*In $4s^24f\ ^2F$ we have used $5f_1^2(^1S)4f_1\ ^2F$

D. $4s4p^2\ ^2D$

All configurations after $4s_24p_2^2\ ^2D$ in B.

included. Because of the cancellation in the transition probability, it is very important to get a good representation of the perturber. According to Fano,[9] the "unperturbed" position of $4s4p^2\ ^2D$ can be observed as the "midpoint" of an absorption resonance in the continuum. That is, the energy distance between our full MCHF calculation for the $nd\ ^2D$ states and the perturber, without the interactions with the d series included, should agree with experimentally obtained energy differences between the bound ^2D states and the position of the resonance profile for $4s4p^2\ ^2D$. To test how sensitive our results were to the agreement in energy differences between theory and experiment, we performed four different types of calculations (denoted I–IV below).

Since the inclusion of extra correlation within the $4s^2$ shell only affects the Rydberg states, and not the perturber, we tested two different representations. First, including the complex of $4s^2$, we used the set

$$(4s^2+4p^2+4d^2+4f^2)^1S$$

in calculations I and III. Then, in calculations II and IV the $5s^2$ configuration was also included in the representation of the ^1S core. A consistent approach for calculation of transition energies demands that the same representation be used for the "core" in both the initial and final state, thus an additional configuration had to be included in all states.

Similarly, relativistic effects contribute to the energy of the ^2D series and the perturber in different ways. The Darwin term, mass correction, and spin-spin-contact term, which are J-independent contributions to the energy matrix, mainly affect the s electrons. Therefore they will contribute more to the energies of the $4s^2nd$ configura-

TABLE II. Schematic description of the different types of calculations.

Calculations	Relativistic effects included	$5s^2nl$ included
I	No	No
II	No	Yes
III	Yes	No
IV	Yes	Yes

TABLE III. Contribution to the $\langle 4s^24p\ ^2P \mid E1 \mid \text{“}4s^2nd\text{”}\ ^2D\rangle$ matrix element. From calculation IV (see text).

n	$c_1\langle 4s^24p \mid E1 \mid 4s^2nd\rangle$	$c_2\langle 4s^24p \mid E1 \mid 4s4p^2\rangle$	Total $S^{1/2}$
4	3.5652	−0.6040	3.0009
5	1.6196	−0.6137	1.0223
6	0.9079	−0.5509	0.3658
7	0.5584	−0.4791	0.0865
8	0.3665	−0.4137	−0.0405
9	0.2507	−0.3518	−0.0956
10	0.1832	−0.3051	−0.1168
11	0.1324	−0.2614	−0.1246

tions than to $4s4p^2$, which has only one occupied $4s$ orbital. In calculation III these relativistic effects are included as perturbations, after the optimization of the orbitals, in calculation I. In the same way calculation IV represents an inclusion of these effects in calculation II. Table II describes the different types of calculations schematically.

Since we have to find a finite expansion for each ^2D state, the important question is: How do we select the right configurations to include? The mixing between the $4s^2nd$ series and $4s4p^{2\,2}D$ results in a cancellation in the transition matrix element around $n=8$, thus the lifetimes of these states are very sensitive to small changes in the contributions to the oscillator strengths. Hence, it is not sufficient only to consider the magnitude of the mixing coefficients in the MCHF representation of the Rydberg states, and reject all configurations with small weights. Some configurations with small weights may be important in determining the position of the perturber. Since the weight of the perturber will depend strongly on a good representation of its correlations, a separate calculation was performed for $4s4p^{2\,2}D$, without including the s^2nd states. The energy of this "unperturbed" state should correspond to the position of the observed absorption resonance in the continuum, as discussed above.

III. DISCUSSION AND RESULTS

In an unperturbed Rydberg series the lifetimes increase smoothly as $(n^*)^3$, but the presence of a perturber may cause an irregular behavior. The mixing between the perturber and the $4s^2nd\,^2D$ states results in two different contributions to the transition matrix element between the ground state and the d states. The transition element is given, approximately, by the expression

$$\begin{aligned}\langle 4s^2 4p\,^2P \,|\, E1 \,|\, \text{“}4s^2nd\text{”}\,^2D\rangle &= c_1\langle 4s^2 4p\,^2P \,|\, E1 \,|\, 4s^2nd\,^2D\rangle \\ &\quad + c_2\langle 4s^2 4p\,^2P \,|\, E1 \,|\, 4s4p^{2\,2}D\rangle\ . \end{aligned} \tag{1}$$

These two contributions have opposite signs and different n dependence. In the first, the transition integral decreases with increasing n because of the decreasing overlap between the $4p$ and the nd wave functions. In the second, the c_2 coefficient can be written approximately as

$$c_2 = \langle 4s^2nd\,^2D \,|\, V \,|\, 4s4p^{2\,2}D\rangle/\Delta E_n\ , \tag{2}$$

where ΔE_n is the energy difference between the perturber and the nd Rydberg state. Analogous to the integral in the first term, the absolute value of the numerator de-

TABLE IV. Observed and calculated distances between the perturber, $4s4p^{2\,2}D$ and the $4s^2nd\,^2D$ states, and oscillator strengths for $4s^24p\,^2P$–$4s^2nd\,^2D$ transitions. In each group the first entry is the energy distance in cm^{-1}, the second the oscillator strength in length form, and the third the oscillator strength in velocity form.

	Calculations				Others[a]	
n	I	II	III	IV	Ref. 4	Ref. 8
4	17 131	17 317	18 916	19 148	18 980[b]	19 420[b]
	0.280	0.284	0.299	0.301		
	0.279	0.279	0.300	0.302		
5	11 083	11 273	12 926	13 174	12 950[b]	13 400[b]
	0.0313	0.0336	0.0393	0.0413		
	0.0315	0.0328	0.0409	0.0424		
6	8278	8476	10 104	10 334	10 180[b]	10 630[b]
	0.0017	0.0024	0.0047	0.0057		
	0.0018	0.0024	0.0057	0.0067		
7	6751	6954	8599	8827	8690[b]	9140[b]
	0.000 38	0.000 10	0.000 10	0.000 33		
	0.000 29	0.000 08	0.000 35	0.000 67		
8	5829	6037	7694	7915	7790[c]	8240[c]
	0.0021	0.0013	0.000 27	0.000 07		
	0.0019	0.0012	0.000 06	0.000 00		
9	5232	5442	7112	7336	7210[c]	7660[c]
	0.0031	0.0022	0.000 75	0.000 47		
	0.0028	0.0020	0.000 35	0.000 16		
10	4824	5037	6715	6938	6820[c]	7270[c]
	0.0032	0.0025	0.000 98	0.000 63		
	0.0029	0.0023	0.000 53	0.000 32		
11	4533	4748	6430	6658	6540[c]	6990[c]
	0.0032	0.0024	0.001 03	0.000 72		
	0.0030	0.0023	0.0062	0.000 40		

[a]Energy of the perturber from experiment (Ref. 4) and semiempirical quantum-defect theory (Ref. 8).
[b]Energies of nd states from Ref. 12.
[c]Energies of nd states from Ref. 14.

creases with increasing n, because of the decreasing overlap between the $4p^2$ and the $4snd$ pairs, but since the perturber is situated above the entire Rydberg series, ΔE_n also will decrease. This causes the absolute value of the first term in (1) to decrease faster than the second, as can be seen in Table III. Their different signs will therefore give rise to a pronounced cancellation for some value of n. For high n the Rydberg states are very closely spaced, so the numerator decreases faster than the denominator and the second term will eventually start to decrease also (see Table III). From Table III it is also obvious that the single-configuration approach, used in Ref. 7, is not valid for higher ^2D states since it does not take the effect of the perturber into account. The different calculations predict different relative positions of the perturber and the Rydberg states, and thereby also different positions for the minimum in transition probabilities. The separations, which are listed in Table IV, increase in going from calculation I to calculation IV, with the experimental value of Kozlov and Startzev[4] being between that of III and IV. The value derived from the semiempirical quantum-defect theory by Neijzen and Dönszelmann[8] is slightly above that of calculation IV.

After the minimum, which is equivalent to the minimum in the Beutler-Fano profile of $4s\,4p^{2\,2}D$, the total probability for the $4s^24p\,^2P$—$4s^2nd\,^2D$ transition will increase. The contribution to the matrix element in (1) from the second term will dominate as the first decreases. Becasue of the broadness of the resonance profile the exact position of the perturber is not known, but Kozlov and Startzev give a wavelength of 1860 Å for the multiplet $4s^24p\,^2P$—$4s\,4p^{2\,2}D$. The energy differences between the $4s^2nd\,^2D$ states and the perturber derived from this wavelength are given in Table IV under the heading "ob-

TABLE V. Transition energies in cm^{-1} (observed and calculated), and transition probabilities, in s^{-1}, for $4s^24p\,^2P$—$4s^2nd\,^2D$. (Only transition probabilities contributing more than 1% to the lifetime for a d state or with $A > 10^4$ are listed.) Calculated transition probabilities are scaled with experimental transition energies. In each group the first and second entries are experimental and theoretical transition energies, respectively, and the third and fourth give transition probabilities from method III and IV (see text).

Lower \ Upper	$4d$[a]	$5d$[a]	$6d$[a]	$7d$[a]	$8d$[c]	$9d$[c]	$10d$[c]	$11d$[c]
$4s^24p\,^2P$[a]	34 235	40 257	43 028	44 523	45 420	45 998	46 391	46 671
	33 197	39 186	42 009	43 514	44 419	45 000	45 397	45 682
	1.45(8)[e]	2.62(7)	3.56(6)	8.44(4)	2.28(5)	6.49(5)	8.67(5)	9.18(5)
	1.46(8)	2.76(7)	4.32(6)	2.67(5)	6.24(4)	3.60(5)	5.52(5)	6.39(5)
$4s^25p\,^2P$[a]	1667	7690	10 460	11 956	12 853			
	1136	7126	9948	11 453	12 358			
	2.73(5)	1.30(7)	5.61(6)	2.58(6)	1.27(6)			
	2.74(5)	1.32(7)	5.74(6)	2.70(6)	1.37(6)			
$4s^26p\,^2P$[a]		404	3174	4670	5567			
		77	2899	4404	5309			
		1.68(4)	3.01(6)	1.42(6)	7.39(5)			
		1.83(4)	3.08(6)	1.44(6)	7.57(5)			
$4s^27p\,^2P$[a]				1618	2515			
				1421	2326			
				1.05(6)	4.88(5)			
				1.06(6)	4.91(5)			
$4s^28p\,^2P$[b]					931			
					5.23(5)[d]			
					5.23(5)[d]			
$4s^24f\,^2F$[a]			2124	3620	4517			
			2044	3549	4454			
			3.51(5)	1.32(5)	6.79(4)			
			3.77(5)	1.28(5)	6.69(4)			
$4s^25f\,^2F$[a]				1119	2016			
				1066	1971			
				2.73(5)	1.00(5)			
				2.57(5)	9.83(4)			
$4s^26f\,^2F$[a]					658			
					622			
					1.74(5)			
					1.62(5)			

[a]Reference 12.
[b]Reference 13.
[c]Reference 14.
[d]Obtained by extrapolation of probabilities for the $np\,^2P$—$nd\,^2D$ transitions, $n = 4$—7.
[e]$p(q)$ implies $p \times 10^q$.

served." As a crude estimate of the uncertainties in this value for the excitation energy of the perturber, the separation between the two lines $4s^2 4p\ ^2P_{1/2}$—$4s\,4p^2\ ^2D_{3/2}$ and $^2P_{3/2}$-$^2D_{5/2}$ may be used. This separation is given by the differences in fine-structure splitting of the two terms involved. For $4s\,4p^2\ ^2D$ Neijzen and Dönzelmann[8] derive $E(\frac{5}{2}-\frac{3}{2})\approx 165\ \text{cm}^{-1}$ and for the ground state we have[14] $E(\frac{3}{2}-\frac{1}{2})=826\ \text{cm}^{-1}$. From this the separation between the two lines is $d\approx 660\ \text{cm}^{-1}$. In Fig. 1 the experimental position of the perturber is shown with these estimated errors. In Table IV, the oscillator strengths for the $4s^2 4p\ ^2P$—$4s^2 nd\ ^2D$ transitions are listed, together with the different methods. The inclusion of J-independent relativistic effects are seen to lower the energy of the Rydberg states more than the energy of the perturber, thereby increasing the distance between them. The inclusion of the $5s^2 nd\ ^2D$ configuration states will depress the Rydberg series similarly, but this represents a much smaller effect. In Fig. 1, the trends for $f_e=(n^*)^3 f$, the effective oscillator strength,[15] are shown for calculations I and III. It is obvious from these curves that relativistic effects lower the energy of the Rydberg states, increase the $4s^2 4d$-$4s\,4p^2$ distance, and shift the position of the oscillator-strength minimum towards higher n values. A comparison of the four calculations shows how sensitive the resulting transition properties are to a good representation of the $4s\,4p^2\ ^2D$ state.

For transitions to ^2F and excited ^2P states the contribution from the second term in (1) is zero since the transition to these states from $4s\,4p^2\ ^2D$ is forbidden. The mixing of $nd\ ^2D$ states with the perturber, therefore, will affect only the c_1 coefficient in the expression

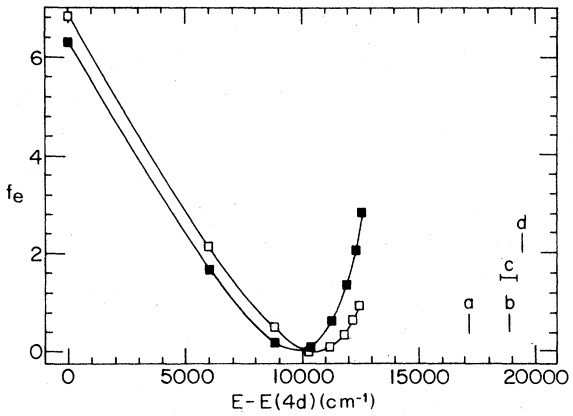

FIG. 1. Effective oscillator strengths for the $4s^2 4p\ ^2P$—$4s^2 nd\ ^2D$ transitions as a function of the energy of the nd states relative to $4d$. ■, nonrelativistic, calculation I (see text); □, relativistic, calculation III (including relativistic shifts, see text); Also indicated is the position of the perturber, $4s\,4p^2\ ^2D$, as obtained from a, nonrelativistic calculation I (see text); b, relativistic calculation III (including relativistic shifts, see text); c, Kozlov and Startzev (Ref. 4); d, Neijzen and Dönszelmann (Ref. 8).

$$\langle 4s^2 mp\ ^2p \mid E1 \mid \text{“}4s^2 nd\text{”}\ ^2D\rangle = c_1\langle 4s^2 mp\ ^2P \mid E1 \mid 4s^2 nd\rangle\ ^2D\ ,\quad m>4\ . \tag{3}$$

In Table V the A values for all transitions contributing to the lifetimes of the ^2D states, together with the corresponding transition energies, are reported. The calculated

TABLE VI. Lifetimes for $4s^2 nd\ ^2D$ states in nanoseconds.

	$4d$	$5d$	$6d$	$7d$	$8d$
Calculated					
I[a]	7.36	29.7	100.1	180	220[b]
II[a]	7.25	28.3	92.1	182	224[b]
III[a]	6.88	25.5	79.7	180	278[b]
IV[a]	6.82	24.5	74.2	169	282[b]
Observed					
Ref. 1	7.4±0.3	29±3	69±7	150±20	270±30
Other					
Calculated					
Ref. 5	6.90[c]				
Ref. 6	6.27[c]				
Ref. 7 $j=\frac{1}{2}$	7.08	12.7	24.1	41.5	80.7
$j=\frac{3}{2}$	7.20	13.0	24.7	42.7	82.6
Observed					
Ref. 7 $j=\frac{1}{2}$	5.8±0.6	16±2	32±3		
$j=\frac{3}{2}$	5.8±0.6	15±2	32±3		

[a]Calculations reported here (see text).
[b]Includes transition probability for $8p\ ^2P$—$8d\ ^2D$ extrapolated from the trend of $np\ ^2P$—$nd\ ^2D$ transition probabilities ($n=4$—7).
[c]Transition to $5p\ ^2P$ not included.

lifetimes, obtained by methods III and IV, confirm the most recent experimental results,[1] especially for states with energy close to the minimum ($n=6$–8). The theoretical transition probability for the $8p\,^2P$–$8d\,^2D$ transition was estimated from an extrapolation of probabilities for np-nd ($n=4$–7) transitions. When this estimate is included in calculation IV, the calculated lifetimes for the most critical states, $n=6$–8, are within the error bars of the experimental results (see Table VI). More important, the results reported here follow the same trend along the sequence as experiment, while the single-configuration approach[7] breaks down for $n>4$.

IV. CONCLUSION

In this paper we have shown that the $4s\,4p^2\,^2D$ perturber has a pronounced effect on the probabilities for transitions from the ground state to members of the $4s^2nd$ Rydberg series, and even causes an almost complete cancellation for $n=7$–9.

The different types of calculations, which give different positions for the perturber relative to the Rydberg series, demonstrate the sensitivity of the oscillator strengths to a "correct" representation of an important perturber. Therefore, in calculations of lifetimes, this type of perturber, and its associated correlation, has to be included in an accurate manner.

ACKNOWLEDGMENTS

This research was supported by the U.S. Department of Energy (Office of Basic Energy Sciences) under Contracts No. DE-AS05-80ER10618 and No. W-31-109-Eng-38 and by the Swedish National Science Research Council (NFR).

---

*Permanent address: Department of Physics, University of Lund, Sölvegatan 14, S-223 62 Lund, Sweden.

†Permanent address: Computer Science Department, Vanderbilt University, Nashville, TN 37235.

[1] J. Carlsson, H. Lundberg, W. X. Peng, A. Persson, C.-G. Wahlström, T. Brage, and C. Froese Fischer, Z. Phys. D **3**, 345 (1986).

[2] C. Froese Fischer, Phys. Scr. **23**, 38 (1981).

[3] C. Froese Fischer and M. Godefroid, Nucl. Instrum. Methods **202**, 307 (1982).

[4] M. G. Kozlov and G. P. Startzev, Opt. Spectrosc. **24**, 3 (1968).

[5] K. Aashamar, T. M. Luke, and J. D. Talman, J. Phys. B **16**, 2695 (1983).

[6] J. Migdalek and W. E. Baylis, J. Phys. B **12**, 2595 (1979).

[7] A. Lindgård, S. Mannervik, B. Jelenkovic, and E. Veje, Z. Phys. A **301**, 1 (1981).

[8] J. H. M. Neijzen and A. Dönszelmann, Physica **114C**, 399 (1982).

[9] U. Fano, Phys. Rev. **124**, 1866 (1961).

[10] J. P. Connerade and M. A. Baig, J. Phys. B **14**, 29 (1981).

[11] C. Froese Fischer, U.S. Department of Energy Report No. Doe/ER/10618-11, 1983 (unpublished).

[12] I. Johansson and U. Litzén, Ark. Fys. **34**, 573 (1967).

[13] G. Jönsson, C. Levinson, I. Lindgren, A. Persson, and C.-G. Wahlström, Z. Phys. A **322**, 351 (1985).

[14] C. Moore, *Atomic Energy Levels,* Natl. Bur. Stand. (U.S.), Natl. Stand. Ref. Data Ser. No. 35 (U.S. GPO, Washington, D.C., 1971), Vol. II.

[15] K. T. Cheng and C. Froese Fischer, Phys. Rev. A **28**, 2811 (1983).